Intergranular Stresses in ZIRCALOY-2

T.M. HOLDEN, R.A. HOLT, and J.W.L. PANG

The development of the understanding of the intergranular stresses in ZIRCALOY-2 is reviewed. Neutron diffraction measurements of the intergranular strains were made on rod-textured material and highly textured plate. The elastoplastic self-consistent (EPSC) model provides a sound theoretical foundation for our understanding of the behavior. The strain response of ZIRCALOY-2 to applied tensile stress is well described for two very different textures with the same slip and hardening parameters. It is almost certain that tensile twinning is the explanation for the response to compressive stress and rolling that is, as yet, incompletely understood.

I. INTRODUCTION

RESIDUAL stresses are generated when samples undergo inhomogeneous plastic deformation. The stresses occur on three length scales. First, a macroscopic stress field, or type 1 stress, of primary interest to the engineer since it may lead to the failure of a component, has a length scale of the same size as the part. In the absence of an applied stress, the residual stresses in the part are in equilibrium. Second, whenever polycrystalline metals are loaded beyond the yield point, the anisotropy of the plastic and elastic deformation of the grains, for grains of different crystallographic orientation, always generates residual stresses. In this case, the stresses and the corresponding strains are different for each grain orientation and are termed intergranular, or type 2 stresses. The spatial scale of these stresses is of the order of the grain size. In a small volume of material sufficient to contain many grains, the intergranular stresses for different grain orientations balance each other and a measurement with a strain gauge is not sensitive to the effect. Only techniques, such as diffraction, which single out particular reflections and, hence, grain orientations, are sensitive to type 2 stresses. Finally, there are strain fields associated with extended defects within grains (type 3 effects), and these have a spatial scale on the order of 1000s of Å. Type 1 stresses give rise to shifts in the diffraction peaks, as do type 2 stresses. In addition, because the response of different crystal orientations that present a given plane normal in a certain direction does vary, type 2 stresses also lead to line broadening. Type 3 stresses contribute to line broadening only. In this review, the emphasis is on using the intergranular strains, deduced from the shifts in diffraction lines, to learn about the deformation processes that have occurred. Since diffraction methods only measure elastic strains, a theoretical model is needed that considers both elastic and plastic deformation in the grains under applied stress. Then, the measured elastic strains may be compared with the theoretical elastic strains in order to deduce the behavior. Basically, with the aid of an interpretive model, the intergranular strains provide information about the dislocations in the material on a statistical basis and, hence, are of interest in this symposium.

The engineering consequences of intergranular stresses and strains in materials exhibiting strong texture can be severe. ZIRCALOY-2* tubing is used extensively in nuclear reactors. In the presence of a flux of fast neutrons, the intergranular strains are relieved in the grains, and as a result, the tubing grows along its length and contracts radially. The role of intergranular strains in the irradiation growth of ZIRCALOY-2 in a fast neutron flux was recognized by Holt and Causey,[1] who developed an early model for the stresses based on the elastic and plastic properties of the grains and the crystallographic texture. The practical interest in the behavior of ZIRCALOY-2 in the calandria tubes of CANDU* reactors at Atomic Energy of Canada Limited lead to extensive experimental and theoretical efforts to measure and understand intergranular stresses in this material. These efforts are reviewed here.

The intergranular strains generated by applied stress can be very large in ZIRCALOY-2 where the **c** axis, [0002], is plastically and elastically stiffer than the orthogonal $[\bar{1}2\bar{1}0]$ and $[10\bar{1}0]$ axes in the basal plane. In addition, the coefficient of thermal expansion along the **c** axis is twice as high as it is in perpendicular directions within the basal plane. This always generates thermal residual strains on cooling from temperatures at which the material is processed or heat treated. The existence of a prior texture affects both the thermal and mechanically induced strains. For example, in a sample direction where the grain orientations are mainly $\langle\bar{1}2\bar{1}0\rangle$ or $\langle 10\bar{1}0\rangle$, which have similar elastic and plastic properties and there are no constraining $\langle 0002\rangle$ grain orientations, the residual strains are small. In directions where there are populations of plastically stiff and plastically soft grain orientations, the residual strains are large.

*ZIRCALOY is a trademark of Westinghouse Electric Company, Pittsburgh, PA.

*CANDU is a trademark of Atomic Energy of Canada Limited.

T.M. HOLDEN, Wheatley Scholar, Los Alamos Neutron Science Center, and J.W.L. PANG, Staff Scientist, Metals and Ceramics Division, are with Oak Ridge National Laboratory, Oak Ridge, TN 37831-6118. Contact e-mail: tmholden@lanl.gov or holdent@magma.co R.A. HOLT, Director, is with the Fuel Channels Division, Atomic Energy of Canada, Ltd., Chalk River, ON, Canada K0J 1P0.

This article is based on a presentation made in the symposium entitled "Defect Properties and Mechanical Behavior of HCP Metals and Alloys" at the TMS Annual Meeting, February 11–15, 2001, in New Orleans, Louisiana, under the auspices of the following ASM committees: Materials Science Critical Technology Sector, Structural Materials Division, Electronic, Magnetic & Photonic Materials Division, Chemistry & Physics of Materials Committee, Joint Nuclear Materials Committee, and Titanium Committee.

REPRODUCED BY PERMISSION OF THE MINISTER OF SUPPLY AND SERVICES CANADA

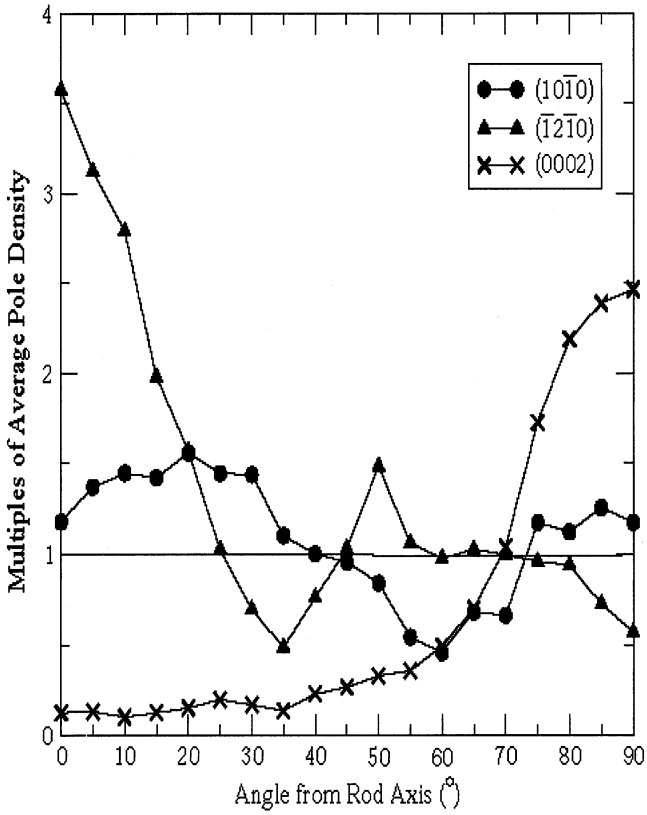

Fig. 1—The variation of texture along a radius of the cylindrically symmetric pole figures for the (10$\bar{1}$0), (0002), and ($\bar{1}$2$\bar{1}$0) reflections of rod-textured ZIRCALOY-2 as measured by Pang *et al.*[8]

II. RESIDUAL STRAIN EXPERIMENTS

A. *Rod-Textured ZIRCALOY-2*

The first experiments on intergranular strains in ZIRCALOY-2 were carried out on rod samples by MacEwen *et al.*,[2] who examined the effect of cooling from elevated temperatures. The pole figures for the ZIRCALOY-2 rod exhibit complete cylindrical symmetry.[3] Two thirds of the grains have ⟨$\bar{1}$2$\bar{1}$0⟩ and one third have ⟨10$\bar{1}$0⟩ crystallographic orientations along the rod axis, while grains with ⟨0002⟩ axes are confined to within about ±35 deg of the equatorial plane of the rod. The variation of the crystallographic texture along a radius of the pole figure for the ⟨10$\bar{1}$0⟩, ⟨$\bar{1}$2$\bar{1}$0⟩, and ⟨0002⟩ reflections is summarized in Figure 1. The strains corresponding to a given grain orientation, say ⟨0002⟩, in a certain sample direction, are obtained from the shifts in the corresponding (0002) diffraction peak in that direction. The thermal strains were found to be low, parallel to the rod axis, since the elastic and plastic properties of all the grains are the same in this direction. However, the strains are large perpendicular to the rod axis where, in any direction in the equatorial plane of the sample, grains with ⟨10$\bar{1}$0⟩ and ⟨$\bar{1}$2$\bar{1}$0⟩ crystal axes are constrained by grains with ⟨0002⟩ axes in the same direction.

Next, the residual strains were measured in ZIRCALOY-2 rod samples that had been deformed in tension to a total of 1, 2, 3, and 4 pct by MacEwen *et al.*[4] After tensile deformation, the strain, in ⟨0002⟩ grains perpendicular to the rod axis, shifts in a compressive sense by -20×10^{-4} and, in ⟨10$\bar{1}$0⟩ grains, shifts in a tensile sense by $+20 \times 10^{-4}$. MacEwen *et al.*[2,4] also showed that the variation of strain for grains with orientations normal to the [$\bar{1}$2$\bar{1}$0] crystal axis followed a simple tensor form.

The elastoplastic self-consistent (EPSC) model was developed by Turner and Tome[5] to describe the preceding experimental results. The model treats each grain orientation as an Eshelby inclusion in a matrix that has the average properties of all the grains. The deformation of each grain is calculated from the operating slip systems, as well as the single-crystal elastic constants. An aggregate of 2000 to 5000 grains is selected whose orientations reproduce the experimental texture of the material. The critical-resolved shear stresses and hardening behavior are usually chosen to match the experimental macroscopic stress-strain curve, and the model is then used to calculate residual strains with no adjustable parameters. The EPSC model described the thermal strains accurately and showed that only elastic accommodation is required. The model also gave a qualitatively correct description of the deformation-induced strains with critical-resolved shear stresses of $\tau^{PR} = 110$ MPa and $\tau^{PY} = 247.5$ MPa for prism and pyramidal slip, respectively, and predicted a critical value for tensile twinning of $\tau^{TT1} = 235$ MPa. Linear self-hardening was assumed in Reference 5, where, for example, the dislocations associated with prism slip do not lock the dislocations associated with pyramidal slip. The values of the hardening coefficients were taken to be twice the value of the critical-resolved shear stresses in the corresponding system, namely, $h^{PR} = 220$ MPa, $h^{PY} = 495$ MPa, and $h^{TT1} = 470$ MPa.

B. *ZIRCALOY-2 Plate*

The crystallographic texture and residual strains in strongly textured, ZIRCALOY-2 rolled plate were investigated in Reference 6. The lattice spacings of the samples were accurately measured, but at that time, the stress-free unconstrained lattice parameters for the samples of ZIRCALOY-2 were not accurately known so that strains were not available. An attempt was made to interpret the data[7] in terms of an upper-bound polycrystalline model. Plastic deformation had to be invoked to explain the thermal residual strains, which is now known to be unnecessary,[5] and the model could not predict the strains after cold rolling without further assumptions. The polycrystalline model, however, did give a reasonable representation of the transient elongation of ZIRCALOY-2 tubes, resulting from radiation-induced creep relaxation of the intergranular strains.

III. IN SITU STRAIN EXPERIMENTS

Recently, the strain response of rod-textured ZIRCALOY-2 to tensile applied stress along the rod axis was examined *in situ* on a neutron spectrometer.[8] The samples were held under load control, and the strain response measured at many applied stresses for three load-unload cycles up to maxima of 0.5, 2, and 5 pct plastic deformation. The *residual* strains agreed with those measured previously,[4] but the new work showed how the strains develop while the sample is under load, and the response was investigated to higher values of plastic deformation. The lattice strains parallel to the applied load were small, as found previously. Perpendicular to the applied stress the strains are large, as

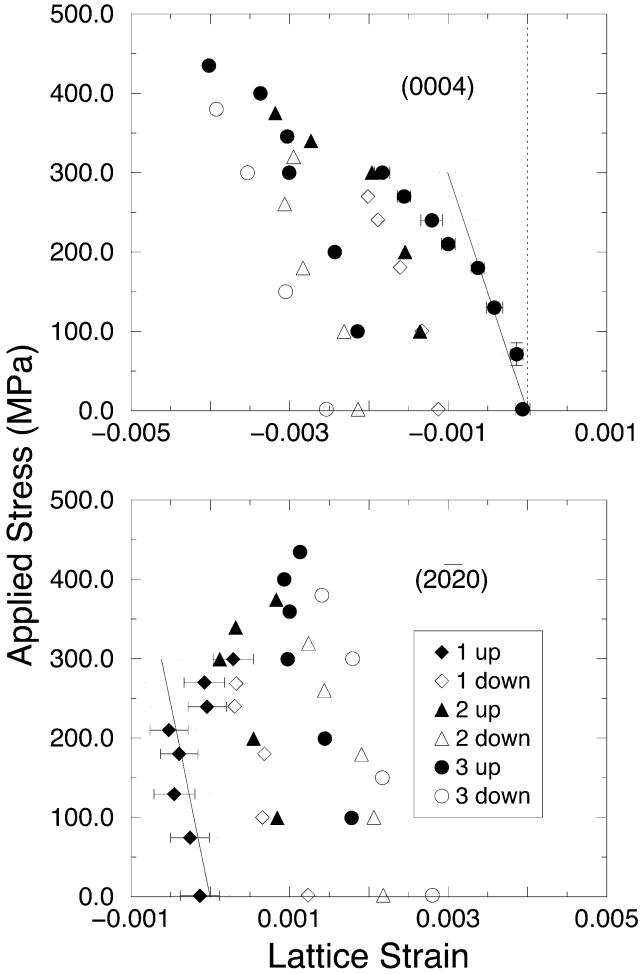

Fig. 2—Transverse lattice strain response as a function of applied stress for the (0004) and (20$\bar{2}$0) reflections of ZIRCALOY-2. The straight lines through the data at the beginning of the first loading cycle are the predicted Poisson linear elastic strain response to applied stress from the EPSC model.

shown in Figure 2 for the (20$\bar{2}$0) and (0004) reflections. Initially, the response follows the Poisson linear-elastic behavior calculated from the texture and the single-crystal elastic constants. However, once slip occurs in $\langle 20\bar{2}0 \rangle$ grains, the $\langle 0002 \rangle$ grains develop larger elastic strains under load than the Poisson response. At this point, compressive transverse stresses appear in $\langle 0002 \rangle$ grains and balancing tensile-transverse stresses appear in $\langle 10\bar{1}0 \rangle$ grains. Figure 2 shows clearly that as the applied stress increases, the strain in $\langle 10\bar{1}0 \rangle$ grains actually shifts in a tensile fashion under load. Upon unloading, the $\langle 0002 \rangle$ grains are left in compression, and the $\langle 10\bar{1}0 \rangle$ grains remain in tension to maintain stress balance.

The EPSC model was applied[8] to the interpretation of the *in situ* data starting with values of the critical-resolved shear stresses for prismatic and pyramidal slip of 110 and 247.5 MPa found earlier.[5] However, for these parameters, the stress required to produce a total strain of 5 pct was overestimated by 30 pct, compared with the experimental stress-strain curve. In addition, the hardening model was changed to a nonlinear homotetic hardening, which is believed to be more realistic than self-hardening since it accounts for the hardening effect of one slip mode on the others. To simulate the stress-strain curve observed in the *in situ* measurements, the critical-resolved shear stresses had to be adjusted downward to 90 and 170 MPa for prism and pyramidal slip respectively. The calculated intergranular strains were then smaller than the experiment[8] by about 50 pct. In order to solve the problem within the EPSC model, the effect of allowing basal slip was examined and found to give an improved match with the stress-strain curve, compared with the case with prism and pyramidal slip alone. With critical-resolved shear stresses of 90, 160, and 240 MPa for prism, basal, and pyramidal slip, and hardening parameters of 45, 80, and 600 MPa, a reasonable distribution of activated slip systems was found (68 pct prism, 24 pct basal, and 8 pct pyramidal). The calculated intergranular strains were in quite good agreement with the experiment. In general, it is fair to say that the residual strains are not very sensitive to the hardening parameters and, therefore, do not offer a very good way to determine the hardening. The macroscopic flow curve still offers the best avenue for deducing hardening parameters on a statistical basis.

Basal slip was inferred previously from tensile test experiments on single-crystal *zirconium*, of unstated purity, by Akhtar[9] at high temperatures. Martin and Reed–Hill deduced the presence of basal slip as a secondary slip mode from kink bands in polycrystalline zirconium.[10] The polycrystalline zirconium was arc-melted sponge with principal impurities (wt pct) 0.04 iron and 0.09 oxygen. The kink bands appeared to form more readily at high temperatures.

In order to test the basal slip hypothesis further, it was decided to check the EPSC model against the textured ZIRCALOY-2 plate data.[6] Since 1988, the unconstrained lattice parameters of our ZIRCALOY-2 material had been determined with good accuracy.[11] First, the variation of lattice spacings for the set of reflections $\{10\bar{1}0\}$ was measured as a function of temperature. The members of the set display different strains at 298 K since they make different angles with the rolling direction of the plate. By extrapolation to the temperature at which they all became equal to within the experimental accuracy, a stress-free temperature of 898 K was found. The temperature of the sample was kept below 850 K, at which temperature, changes in the microstructure occur. The coefficients of thermal expansion were also remeasured on a high-purity single crystal of zirconium and found to be $\alpha_a = (5.8 \pm 0.1) \times 10^{-6}$ K^{-1} and $\alpha_c = (10.3 \pm 0.2) \times 10^{-6}$ K^{-1}. It was assumed that the coefficients of thermal expansion of ZIRCALOY-2 were identical to those of zirconium. The unconstrained lattice parameters at room temperature were then calculated from the lattice parameters of ZIRCALOY-2 at the stress-free temperature and the coefficients of thermal expansion for zirconium and found to be a_{sf} (298 K) = 3.2306 Å and c_{sf} (298 K) = 5.1496 Å. These values compared well with the lattice parameters of a small crystal of ZIRCALOY-2 found by accident in a polycrystalline boule that indicated values of 3.2306 and 5.1484 Å, respectively.[2] With the values of the reference lattice spacings, it was possible to obtain absolute strains for the plate ZIRCALOY-2 samples and to make a thorough comparison with the EPSC model. An article describing this work fully[12] is in press.

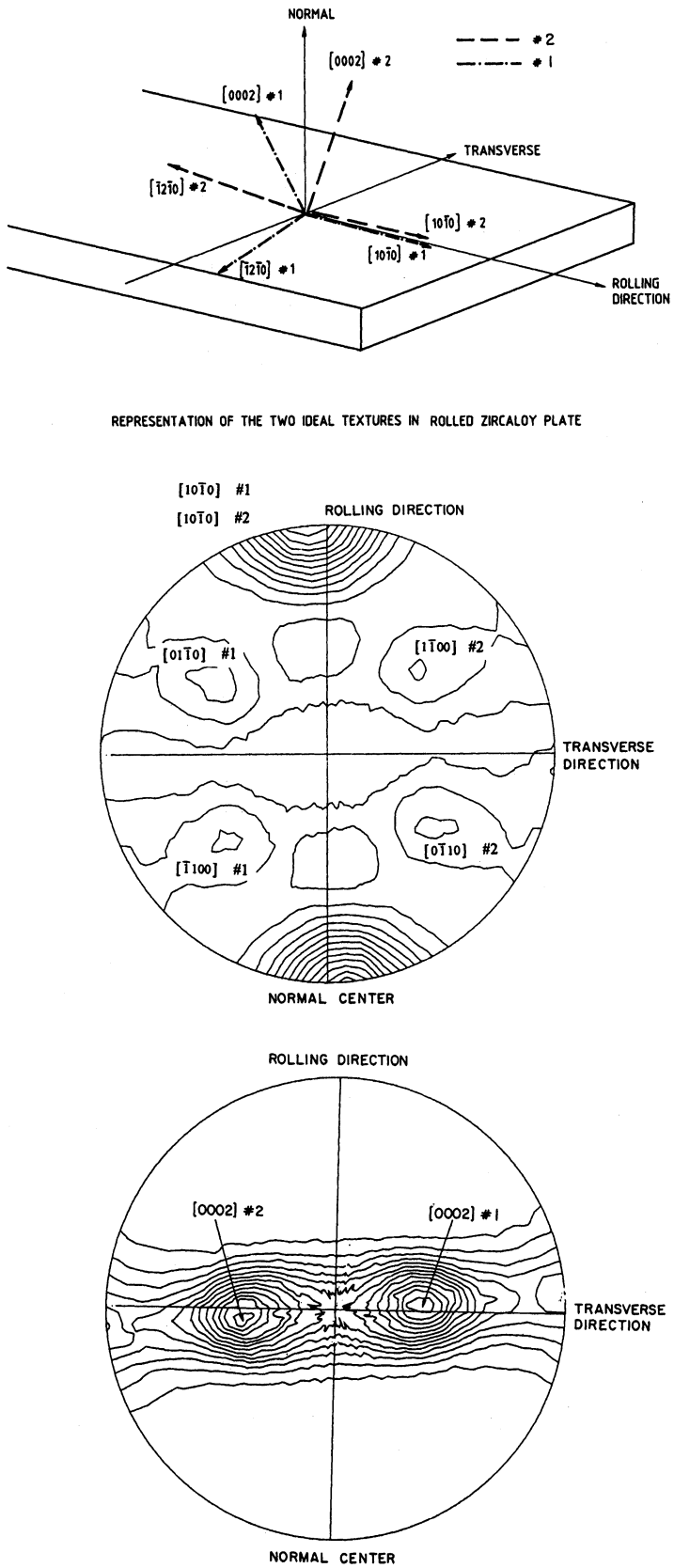

Fig. 3—A schematic representation of the ideal orientation in the ZIRCALOY-2 plate together with the $(10\bar{1}0)$ and (0002) pole figures. In crystal polar coordinates, (θ, φ), ($\theta = 90$ deg, $\varphi = 0$ deg) corresponds to the rolling direction, while ($\theta = 90$ deg, $\varphi = 90$ deg) corresponds to the $[\bar{1}2\bar{1}0]$ orientation of grain 1 located 140 deg clockwise from the labeled transverse direction.

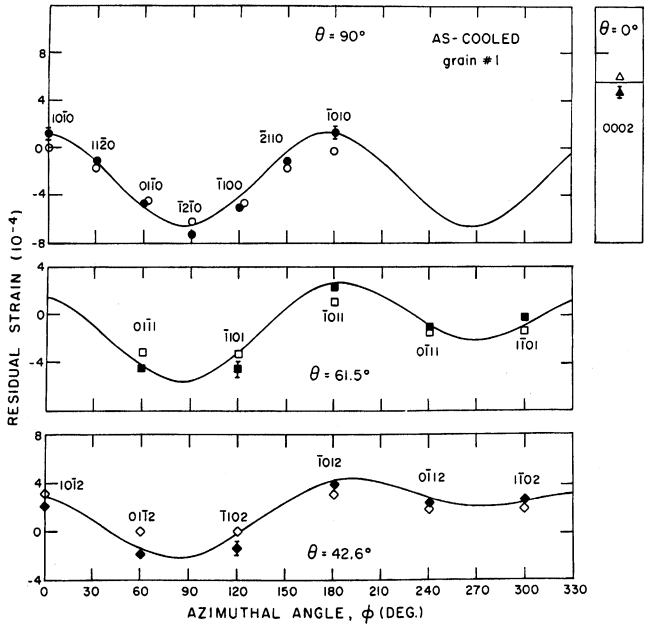

Fig. 4—Residual strains as a function of crystal polar coordinates (θ, φ) for ideal orientation 1 of the as-cooled ZIRCALOY-2 plate. Filled symbols denote experimental data, open symbols the EPSC calculations, and curves the least-squares fit of the experimental data to a tensor form of strain. The data are also labeled by the corresponding (*hkil*) planes in the crystal coordinate system.

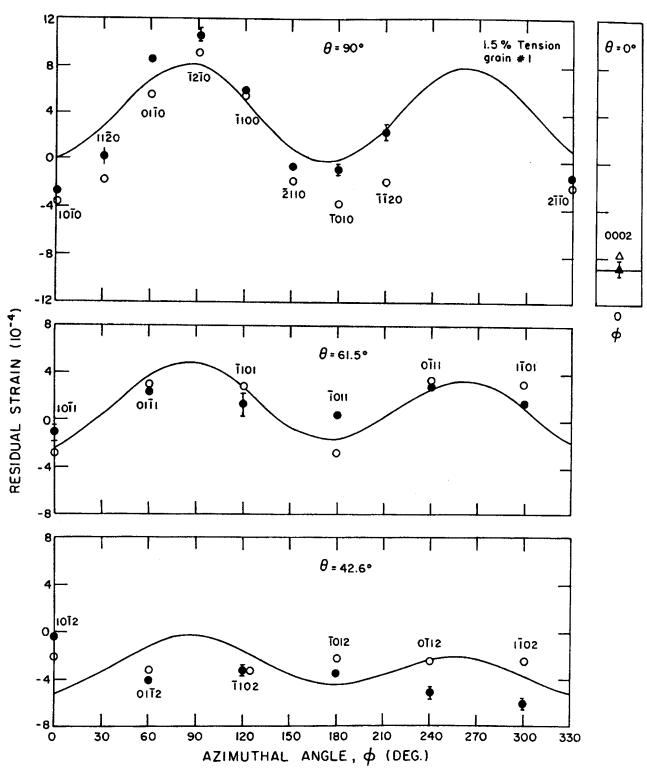

Fig. 5—Residual strains as a function of crystal polar coordinates (θ, φ) for ideal orientation 1 of the ZIRCALOY-2 plate sample deformed in tension by 1.5 pct. Filled symbols denote the experimental data, open symbols the EPSC calculations, and curves the least-squares fit of the experimental data to a tensor form of strain. The data are also labeled by the corresponding (*hkil*) planes in the crystal coordinate system.

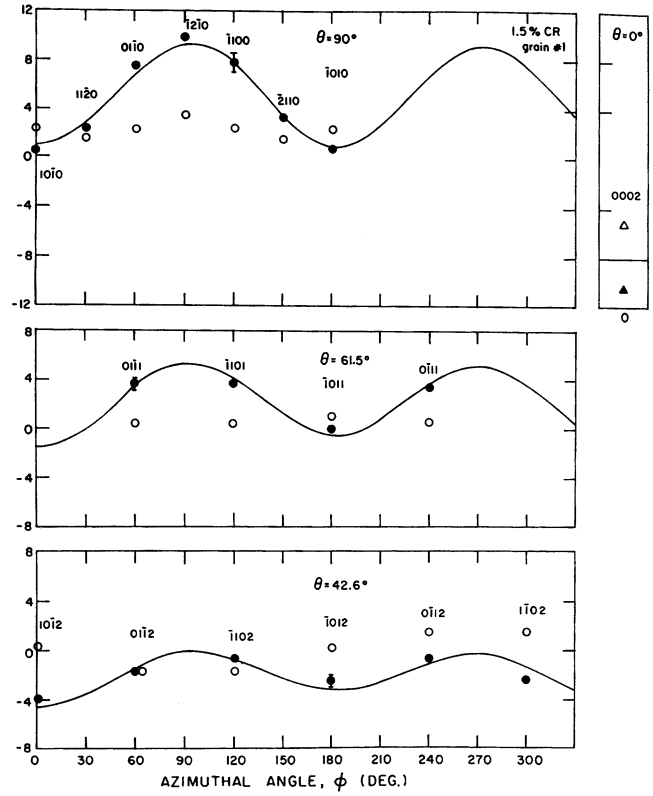

Fig. 6—Residual strains as a function of crystal polar coordinates (θ, φ) for ideal orientation 1 of the ZIRCALOY-2 plate sample cold rolled by 1.5 pct. Filled symbols denote the experimental data, open symbols the EPSC calculations, and curves the least-squares fit of the experimental data to a tensor form of strain. The data are also labeled by the corresponding (*hkil*) planes in the crystal coordinate system.

IV. DISCUSSION OF PLATE-TEXTURED ZIRCALOY-2

The plate had been hot rolled at 1116 K, air annealed for 15 minutes at 1116 K, cooled, and conditioned. The material was subsequently vacuum annealed at 823 K for 1 hour and vacuum cooled to room temperature. In this condition, the "as-cooled" sample displays thermal residual stresses. A second and third sample were reduced in thickness by 1.5 and 25 pct by cold rolling at room temperature. The roll diameter to plate thickness ratio was of an order of 40, and the plate was not constrained at the edges. A fourth sample was subjected to a 1.5 pct tensile deformation along the original rolling direction.

The $(10\bar{1}0)$ and (0002) pole figures for the as-cooled sample are shown in Figure 3 and indicate strong rolling texture with $(10\bar{1}0)$ poles, enhanced five times with respect to a random distribution in the rolling direction. The (0002) poles are concentrated in the normal-transverse plane with the maxima about 40 deg from the normal direction. Figure 3 also shows schematically the two ideal orientations in the plate corresponding to the two maxima in the (0002) pole figures with a common $[10\bar{1}0]$ axis along the rolling direction. These are referred to as the ideal orientations 1 and 2. The presence of strong texture permits a measurement of the intergranular strain tensor for an assembly of grains that have nearly the same orientation because there is a one-to-one correspondence between direction in the sample and crystal orientation. In the $(10\bar{1}0)$ pole figure, Figure 3, every

Table I. Strain Tensors in Units of (10^{-4}) Describing the Strains in the Ideal Orientations of ZIRCALOY-2 Plate

Grain Description	ε_{11}	ε_{22}	ε_{33}	ε_{12}	ε_{23}	ε_{31}
As-cooled grain 1	1.1 ± 0.4	−6.6 ± 0.5	5.6 ± 0.6	−0.5 ± 0.4	−2.1 ± 0.4	−0.7 ± 0.5
As-cooled grain 2	1.4 ± 0.6	−7.4 ± 0.5	5.8 ± 0.6	−0.6 ± 0.3	2.5 ± 0.4	−0.4 ± 0.4
1.5 pct T grain 1	0.0 ± 1.0	7.8 ± 1.3	−9.0 ± 1.3	1.1 ± 0.9	1.0 ± 1.0	−0.4 ± 1.0
1.5 pct T grain 2	0.9 ± 1.6	7.5 ± 1.5	−9.4 ± 1.5	0.5 ± 1.0	−1.1 ± 1.0	0.0 ± 1.1
1.5 pct CR grain 1	1.1 ± 0.5	9.2 ± 0.5	−8.1 ± 0.6	−0.4 ± 0.3	0.1 ± 0.3	−0.6 ± 0.4
1.5 pct CR grain 2	1.7 ± 0.5	9.8 ± 0.3	−9.0 ± 0.5	0.5 ± 0.2	−0.4 ± 0.3	−0.5 ± 0.3
25.0 pct CR grain 1	0.0 ± 0.8	9.9 ± 1.2	−6.8 ± 1.4	−2.3 ± 0.8	6.9 ± 0.8	−1.4 ± 0.8
25.0 pct CR grain 2	0.3 ± 0.7	11.1 ± 0.5	−11.4 ± 0.5	−0.4 ± 0.3	−9.5 ± 0.4	−0.9 ± 0.4

region of high intensity may be identified with a specific crystal orientation for either ideal orientation 1 or 2. It is easy to orient the sample to align particular reflections and, hence, measure the strain tensors for both grains. The logical Cartesian axis system to describe the tensor behavior has principal axes $[10\bar{1}0]$, $[\bar{1}2\bar{1}0]$, and [0002]. The relation between the ideal orientations 1 and 2 and the sample axes is shown in Figure 3. Polar angles (θ and φ) in this coordinate system define the other crystal directions. θ is the angle between the pole of interest and the basal pole, and φ is the azimuthal angle in the basal plane. For example, the poles of the set of reflections, such as $\{10\bar{1}1\}$, make an angle of $\theta = 61.6$ deg with the basal pole in ZIRCALOY-2.

Measurements were made of the $\{10\bar{1}0\}$, $\{20\bar{2}0\}$, {0002}, {0004}, $\{10\bar{1}1\}$, $\{10\bar{1}2\}$, and $\{\bar{1}2\bar{1}0\}$ reflections at specific angles of tilt and orientation, determined from the pole-figures, corresponding to ideal orientations 1 and 2. The residual strains for ideal orientation 1 for the as-cooled, 1.5 pct tension and 1.5 pct cold-rolled samples are shown in Figures 4, 5, and 6 in (θ and φ) coordinates. Solid symbols denote the experimental results, and open symbols represent the EPSC model calculations made with the hardening and critical-resolved shear-stress parameters for the ZIRCALOY-2 rod.[8] The distribution of grain orientations, however, was calculated from the crystallite orientation distribution for rolled ZIRCALOY-2 plate. There was no adjustment of parameters within the EPSC model to describe the results in Figures 4 through 6. The curves in Figures 4 through 6 represent least-squares fits to a general form of a tensor in crystal axis coordinates and give a good representation of the experimental data.

There is close agreement, as shown in Figure 4, between experiment and the EPSC model for the as-cooled sample for ideal orientation 1 (and also for 2 although this is not shown). Elastic processes among the grains alone account for the results, as shown earlier by Turner and Tomé.[5] For the sample deformed in tension by 1.5 pct, the model also agrees with the experiment with no adjustable parameters, as shown in Figure 5. The critical-resolved shear stresses suggested by Pang *et al.*,[8] including basal slip, therefore, appear to be an improvement over those suggested by Tomé *et al.*[11] The strains corresponding to other orientations than the two ideal orientations for the thermal strains and the case of tension are also well described by the EPSC model,[12] although these are not shown here.

Rolling was simulated in the EPSC model by a 1.5 pct compression, and the model calculation for the plate shown in Figure 6 is not in agreement with the experiment. The shifts of the strains away from the thermal stress state have the right sign but are typically too small by 50 pct. As in the previous cases, the strain in the rolling direction remains small relative to the strains perpendicular to the rolling direction.

Twinning, which provides another mode of **c** axis deformation, was not included in the model calculation for the 1.5 pct cold-rolled case. It was shown in the residual strain experiments on the ZIRCALOY-2 rod[3,4] that for less than 2 pct plastic deformation the behavior in compression is opposite to that in tension. The strain in ⟨0002⟩ grains perpendicular to the rod axis initially shifts in a tensile sense under compression. However, at plastic deformations of about 2 pct, a reversal of the initial trend occurs. Tensile twinning of the type $(10\bar{1}2)\langle\bar{1}011\rangle$, when the stress is parallel to the **c** axis of a grain, was invoked[3,4] to explain this reversal. The large texture changes generated by deforming a ZIRCALOY-2 rod in compression[3,4] were consistent with the preceding twinning mechanism operating on the minority set of grains with $\langle 10\bar{1}0\rangle$ directions along the rod axis that comprise about one third of the total number,[3,4] as described in Section II–A.

The strain tensor elements for ideal orientations 1 and 2 are given in Table I. The ε_{11} elements, along the rolling direction, are small and, as explained earlier, the rolling texture is responsible for this feature since there is an overwhelming volume fraction of $[10\bar{1}0]$ grains in this direction. Perpendicular to the rolling direction, [0002] and $[\bar{1}2\bar{1}0]$ grain orientations constrain each other and give the thermally and mechanically induced strains and large values of ε_{33} and ε_{22}. The off-diagonal element, ε_{23}, is sometimes found to be nonzero and changes sign between ideal orientations 1 and 2. This result is a consequence of the symmetry of the rolled plate. Only when there is a change of sign in the off-diagonal element between the two ideal orientations are the strains resolved along the plate normal and transverse directions equal. The maximum and minimum thermal strains, $+4.6 \times 10^{-4}$ and -7.5×10^{-4}, are similar to those found for rod texture by MacEwen *et al.*[2] and Pang *et al.*[8] The tensors for the deformed samples are completely different to those for the cooled sample with changes of sign for ε_{22} and ε_{33}. The changes in the diagonal elements for 1.5 pct tension in units of 10^{-4} are -1.1 ± 1, 14.4 ± 1.8, and—14.6 ± 1.9, and these are similar to the changes generated by tension in rod-textured ZIRCALOY-2.[3,8] The explanation is similar to that for the rod material, namely, that $\langle\bar{1}2\bar{1}0\rangle$ grain orientations slip readily, while ⟨0002⟩ grains first deform elastically.

Figure 7 shows the experimental strain tensors for the ideal orientations 1 and 2, plotted in a pole figure representation for the as-cooled sample. It is worth noting that the tensile strain in the $[\bar{1}2\bar{1}0]$ direction for ideal orientation 2 occurs in nearly the same direction as the compressive [0002]

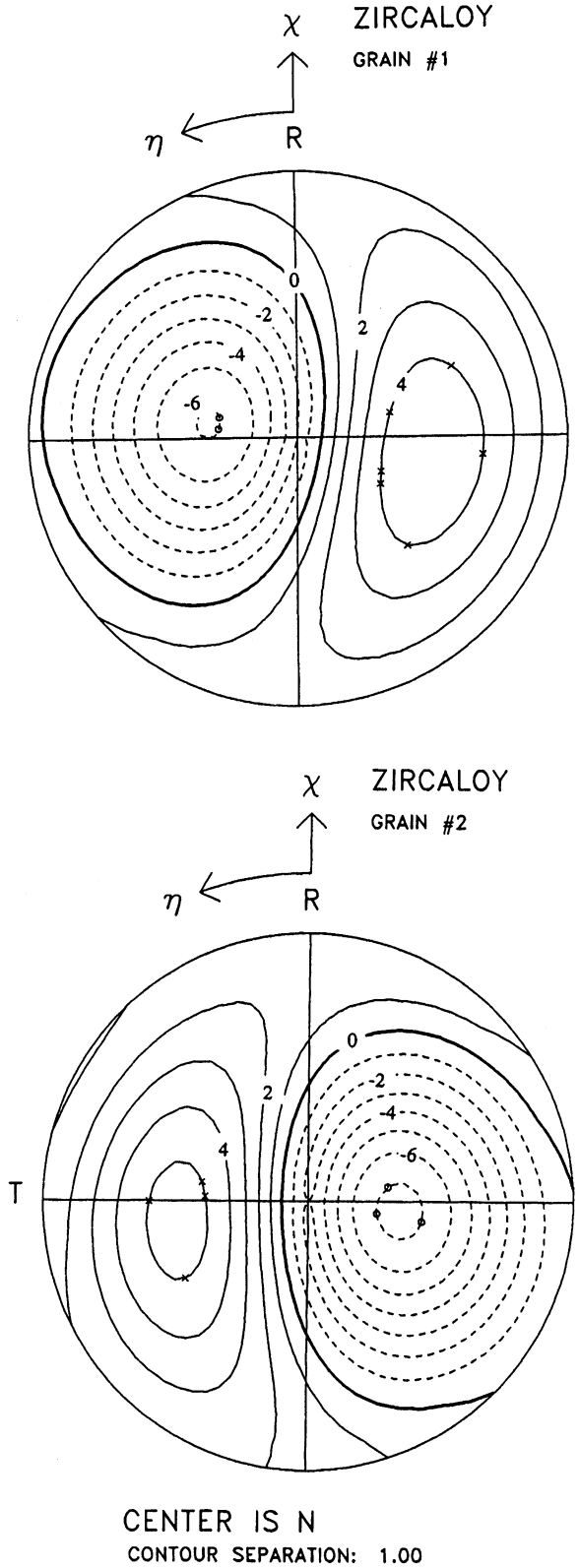

Fig. 7—Strain tensors derived from the fits to the strain data for ideal orientations 1 and 2 for the as-cooled sample plotted in a pole-figure representation.

strain for orientation 1. Since ZIRCALOY-2 is not very anisotropic elastically, this implies that stress balance is achieved by the balance of the [0002] grains in orientation 1 against the $[\bar{1}2\bar{1}0]$ grains in orientation 2. The strains along the sample principal axes, the rolling, transverse, and normal directions, are small. If the measurements had been restricted to the sample principal axes, the large intergranular effects would have been missed since the largest strains tend to be close to principal crystal axes, as was the case for rod-textured ZIRCALOY-2.

V. CONCLUSIONS

The EPSC model gives a very good description of the residual and *in situ* strains in ZIRCALOY-2, as well as the macroscopic stress-strain curves. The set of parameters proposed by Pang *et al.*[8] passes the test of consistency between two quite different textures for the thermal strains and for applied tension. Understanding the strain data for the cold-rolled plate will, almost certainly, require tensile twinning to be incorporated in the EPSC model. *In situ* compression experiments on rod-textured ZIRCALOY-2 to test this hypothesis are in hand.

ACKNOWLEDGMENTS

We acknowledge the valuable contributions made to these studies by C.N. Tomé, J.H. Root, and P.A. Turner.

REFERENCES

1. R.A. Holt and A.R. Causey: *J. Nucl. Mater.*, 1987, vol. 150, pp. 306-18.
2. S.R. MacEwen, C.N. Tomé, and J. Faber, Jr.: *Acta Metall.*, 1989, vol. 37, pp. 979-89.
3. S.R. MacEwen, N. Christodoulou, C.N. Tomé, J. Jackman, T.M. Holden, J. Faber, Jr., and R.L. Hitterman: *Proc. 8th Int. Conf. on the Textures of Materials (ICOTOM8)*, J.S. Kallend and G. Gottstein, eds., TMS, Warrendale, PA, 1988, pp. 825-35.
4. S.R. MacEwen, N. Christodoulou, and A. Salinas-Rodriguez: *Metall. Trans. A*, 1990, vol. 21A, pp. 1083-95.
5. P.A. Turner and C.N. Tomé: *Acta Metall. Mater.*, 1994, vol. 42, pp. 4143-53.
6. T.M. Holden, J.H. Root, V. Fidleris, R.A. Holt, and G. Roy: *Mater. Sci. Forum*, 1988, vols. 27–28, pp. 359-70.
7. R.A. Holt, T.M. Holden, A.R. Causey, and V. Fidleris: *Proc. 10th Risø Int. Symp. on Metallurgy and Materials Science*, J.B. Bilde-Sorensen, N. Hansen, D. Juul-Jensen, T. Leffers, H. Lilholt, and O.B. Pedersen, eds., Risø National Laboratory, Roskilde, Denmark, 1989, pp. 383-89.
8. J.W.L. Pang, T.M. Holden, P.A. Turner, and T.E. Mason: *Acta Mater.*, 1999, vol. 47, pp. 373-83.
9. A. Akhtar: *Acta Metall.*, 1973, vol. 21, pp. 1-11.
10. J.L. Martin and R.E. Reed-Hill: *TMS-AIME*, 1964, vol. 230, pp. 780-85.
11. C.N. Tomé, N. Christodoulou, P.A. Turner, M.A. Miller, C.H. Woo, J.H. Root, and T.M. Holden: *J. Nucl. Mater.*, 1996, vol. 227, pp. 237-50.
12. T.M. Holden, J.H. Root, R.A. Holt, and P.A. Turner: *J. Nucl. Mater.*, (in press).